doi.org/10.36721/PJPS.2020.33.5.REG.1987-1994.1

Comparative study of antibacterial activity between Schiff base nicotinic hydrazide derivative and its silver architected nanoparticles with atomic force microscopic study of bacterial cell wall

Zeba Gul Burki[1], Samiullah Burki[2], Shazia Haider[3], Ijaz Ahmed[3], Mehjabeen[2] and Saba Zafar[1]

[1]HEJ Research Institute of Chemistry, International Center for Chemical and Biological Sciences, University of Karachi, Karachi
[2]Department of Pharmacology, Faculty of Pharmacy, Federal Urdu University of Arts, Science and Technology, Karachi, Pakistan
[3]Department of Pharmaceutical Chemistry, Faculty of Pharmacy ad Pharmaceutical Sciences, University of Karachi, Karachi, Pakistan

Abstract: The threat of multi-drug resistant bacterial pathogens evokes researchers to synthesized safe and effective chemotherapeutic agents for nano-drug delivery system. In current study, Schiff base of nicotinic hydrazide(NHD) and its silver nanoparticles(NHD-AgNPs) were synthesized and characterized. These compounds were investigated for cytotoxicity, antibacterial and AFM activity. The NHD showed LD_{50} at >1000µg/mL while NHD-AgNPs didn't exhibit toxicity at 1000µg/mL against 3T3 cell line. The NHD showed zone of inhibition against two strains of *salmonella enteric* (ATCC 14028 and 700408) 45.29±1.66 and 48.01±1.43mm respectively at 160µg/mL ($p<0.01$) while NHD-AgNPs exhibited 55.87±2.08 and 52.88±1.42 mm respectively at 130µg/mL ($p<0.001$) in disc diffusion method. NHD showed more than 70% growth inhibition for both strains at 85 and 125µg/ml ($p<0.01$) respectively, while NHD-AgNPs inhibit 80% and 75% respectively at 75 and 125 µg/ml ($p<0.01$, $p<0.001$) against Alamar blue antibacterial assay. For morphological changes in bacterial cell wall NHD and NHD-AgNPs treated bacterial cells were observed under atomic force microscope(AFM) and treated bacterial cells were severely damaged with leaked cytoplasmic contents as compare to untreated bacterial cell. These results validate that NHD-AgNPs were highly active as compared to NHD against both strains at their MIC concentrations. In future, comparative wound healing potential will be emphasized.

Keywords: Nicotinic hydrazide Schiff base, silver nanoparticles, cytotoxicity, antibacterial, atomic force microscope.

INTRODUCTION

Bacterial infectious diseases are key contributor to mortality and morbidity, in both developed and developing world. About 60% of total mortality in developing countries, are due to infectious diseases caused by bacterial pathogens. The 3rd principal reason of mortality in Europe, particularly in enervated and aged populations is considered to be due to bacterial pathogen (Vicente *et al*., 2006). Currently used antibiotics are associated with certain drawbacks such as adverse side effects and toxicities. Therefore, search for the discovery of new efficient antibiotics has attracted greater scientific interest (Fauci *et al*., 2005). Moreover, the emergence of multidrug-resistant (MDR) pathogens have noticeably threatened the current chemotherapy. MDR bacterial infections much frequently lead to increase in treatment cost, extended hospitalization and mortality (Marasini *et al.*, 2015). Thus, novel antibacterial drug development with efficient mechanism of action and advanced safety level is noticeably an immediate medical need.

Schiff bases are condensation products of carbonyl compounds with primary amines. In the current era Schiff bases compounds gain high importance. They carry imine or azomethine (-C=N-) functional group and are versatile pharmacophore for the designing and emerging of various pharmacologically lead compounds (Kajal *et al*., 2013). Broadly they are biologically active like as antipyretic, antiviral, antifungal, antibacterial, and antimalarial (Przybylski *et al*., 2009 and Guo *et al*., 2007). Schiff bases have been reported as a promising antibacterial agent. N-(salicylidene)-2-hydroxyaniline is effective against *Mycobacterium tuberculosis* even at the lowest concentration of 8µg/mL (Souza *et al*., 2007). Schiff bases holding 2, 4-dichloro-5-fluorophenyl moiety have also been found effectively inhibit bacterial growth. Schiff bases compounds of this class have been reported for complete inhibition of the growth of *S. aureus, E. coli, P. aeruginosa* and *K. pneumonia* (Karthikeyan *et al*., 2006).

Precision-engineered nano-materials recently, have grab widespread consideration for the progress of novel therapeutic agents and investigative modalities for human use. The unique physicochemical properties and their imperative applications, silver nanoparticles (AgNPs) have established great attention in the arena of nanomedicine research, especially as an antibacterial agent (Gurunathan, 2014). AgNPs achieve a broad spectrum of bactericidal activity against MDR bacteria through their adhesion to bacterial membrane and penetration into the cells, causing various dysfunctions and structural disruptions through production of oxidative

**Corresponding author:* e-mail: zebbarki@yahoo.com

stresses and inhibition of bacterial biofilm formation (Wingender and Flemming, 2010, Donlan, 2002 andWu *et al*., 2014). The antibacterial activity of therapeutic molecules can be improved through their combination with AgNPs. Therapeutically active molecules can be efficiently delivered through bacterial cell wall via their surface conjugation with AgNPs (Shah *et al*., 2014).

This study focuses the Schiff base synthesis of nicotinic hydrazide with 4-hydroxy-3-methoxybenzaldehyde and characterization of Schiff base and its use as capping agent for fabrication of AgNPs. Silver-nanoparticles were explored for their cytotoxicity and antibacterial activity against both sensitive and resistant strains of *S. enterica* (ATCC 14028 sensitive strain, ATCC 700408 (MDR strain). This study was aimed, to investigate in-vitro antibacterial activity through disc diffusion and alamar blue assays. The bactericidal potentials of the synthesized Schiff base capped AgNPs were further authenticated through investigation of surface morphological changes of the bacterial strains using AFM.

MATERIALS AND METHODS

Silver nitrate, nicotinic acid hydrazide, Polylysine (PLL) and sodium borohydride ($NaBH_4$) were procured from Sigma-Aldrich (USA). The solutions were made in deionized water. Nutrient agar, Mueller Hinton agar and Trypton soya broth were obtained from OXOID (UK). Resazurin sodium (RS) salt dye was purchased from Chem-Impex-Int'LInc (USA).

Synthesis of Schiff base (NHD)

The Schiff base were prepared as explained by (Eldehna *et al*., 2015) with slight modification. Briefly, in round bottom flask 68.5mg of nicotinic hydrazine was taken with 20mL ethanol followed by proper stirring. An aldehyde (4-hydroxy-3-methoxybenzaldehyde) in a ratio 1:1 was added to the mixture and refluxed for 12 hrs at 80□, while as a catalyst 1mL glacial acid was used. Periodically the reaction completion was traced by TLC technique. Once the reaction is completed, the reaction was stopped, and cooled through addition of ice-cold water. The precipitated product was collected, filtered and further washed with water and ethanol. The mass and H^1-NMR spectra are given in supplementary file (S1and S2).

Synthesis of Schiff base capped-silver nanoparticles (NHD-AgNPs)

The fabrication of newly synthesized nicotinic hydrazide Schiff base compound coated as a silver nanoparticle as explained by (Shah *et al*., 2014). The aqueous solution of $AgNO_3$ was chemically reduced with $NaBH_4$ using a Schiff base stabilizing agent. Typically, aqueous solution of silver nitrate (1mL of 10^{-3} M) was added in the solution of the synthesized Schiff base (1mL of 10^{-3} M) under constant stirring. Freshly prepared solution of $NaBH_4$ (50µL, 2mM) was added in to the reaction mixture. Specific color change was noticed in solution from pale yellow to brown, after the addition of $NaBH_4$. The solution was stirred for 1h at room temperature. Schiff base coated silver nanoparticles were centrifuge at 14,000 RPM for 20 min. and collected in the form of precipitate. Nanoparticles were redispersed in DI-water for characterization.

Spectral characterization of NHD

Yield: 88.56%, m.p 126-127.6 ºC FT-IR (KBr): 3035 cm^{-1} (OH), 1654 cm^{-1}(C=O), 1599 cm^{-1} (C=C aromatic), 1573 cm^{-1} (C=N-) EI-MS (m/z): 271.10 H^1-NMR (400 MHz, MeOD) δ(ppm):9.04 (1H, d, J=6.7, H-2'), 8.74 (1H, m, H-6'), 8.34 (1H, br, H-4'), 7.55 (3H, m, H-5'; H-5, H-3), 8.74 (1H, s, H-8), 6.87 (1H, d, J=7.8, H-3), 3.30 (3H, s, H-7).

Spectral Characterization of NHD-AgNPs

The characterization of physico-chemical parameters of nanoparticles are essential for their behavior, bio-distribution, safety and efficacy. Therefore, characterization of synthesized silver nanoparticles of NHD is performed via different analytical technique i.e. UV-visible spectroscopy, fourier transform infrared (FTIR) spectroscopy, atomic force microscope (AFM), scanning electron microscope (SEM), dynamic light scattering (DLS) and Zeta potential.

The formation and stability of Schiff base capped silver nanoparticles was confirmed by the distinct surface plasmon resonance (SPR) bands observed in the UV-Visible spectroscopic analysis at 470 nm (fig. 1). To evaluate the stabilization of silver nanoparticles through synthesized Schiff base, FT-IR studies were performed. (fig. 2) represents the comparative FTIR spectra of Schiff base (red trace) and Schiff base coated silver nanoparticles (blue trace). The spectra of Schiff base exhibited the characteristic peaks of functional groups present in its structure. Schiff base displayed peak at 3035 cm^{-1} which corresponds to the stretching vibrational peaks of aromatic C-H bond. Significant stretching vibrational peaks were observed at 1700cm^{-1} and 1607 cm^{-1}which corresponded to the presence of C=O and C=C groups, respectively. After the formation of NH derivative-Ag nanoparticles, peak shifts were observed in the spectrum. Peaks appearing at 1716cm^{-1} and 1509 cm^{-1} indicated the involvement of -CHO group in the stabilization of nanoparticles.

AFM analysis was performed to observe the morphology and average particles height of Schiff base coated silver nanoparticles. (fig. 3a) shows the AFM images of Schiff base coated silver nanoparticles. The topographical image exhibited an array of sharp edge nanoparticles having average particles heights in the range of 55-65 nm. The synthesized nanoparticles are almost spherical, with size

range from 74.3-117 nm as conformed by SEM image (fig. 4). The average particle size observed through SEM was 96.55 nm.

The average particle size distribution and poly dispersity index (PDI) of Schiff base coated silver nanoparticles was evaluated by using dynamic light scattering (DLS) measurements which are given in (fig. 5a). The graph shows the large size distribution of nanoparticles in the range of 25 to 85 nm. PDI of the sample was 0.238 which indicated the poly dispersive nature of the sample having wide range of particles size distribution. To evaluate the stability of nanoparticles in the solution, zeta potential analysis was performed. The graph was shown in (fig. 5b). The zeta potential represents the surface charge acquired by the nanoparticles and it was found to be -16.3 mV. Negative value indicates that the particles have high repulsion which will result in less agglomeration and hence the stability of the nanoparticles solution is increased.

Cytotoxicity bioassay

The synthesized nicotinic hydrazide derivative and its architected nanoparticle was evaluated for toxicity study against normal mouse fibroblast cells using MTT bioassay as reported by (Burki *et al*., 2019). Briefly, the FBS, penicillin and streptomycin supplemented 3T3 cells were incubated with 5% CO_2 at 37°. The cells after grown were harvested, followed by counting on hem-cytometer were transfer in to on flat bottom 96-well plate keeping density at 5×10^4 cells/mL. The plates were re-incubated and the medium was replaced by different concentrations (62.5-1000µg/mL) of synthesized compound and its nanoparticle. After 48 hrs in incubation of 3T3 cells along with different concentration of synthesized compound and its nanoparticles 200µL of MTT (0.5mg/mL) was added to each well followed by re-incubation for 4 hours. To each well 100µL of DMSO was added. The absorbance of MTT to formazan was measured at 540nm.The inhibitory percentage was calculated as;

$$\text{Inhibition (\%)} = 100 - \left| \frac{\text{Mean of O.D. of test compound} - \text{Mean of O.D. negative control}}{\text{Mean of O.D. of positive control} - \text{Mean of O.D. of negative control}} \right| \times 100$$

Antibacterial activity

Bacterial strains collections

The strains of *Salmonella enterica* subsp. *Enterica* serovar Typhimurium (ATCC 700408 and ATCC 14028) were collected from culture bank of International Center for Chemical and Biological Sciences (ICCBS).

Disc diffusion method

The disc diffusion method was used to evaluate the antimicrobial activity of compound and its silver nanoparticles against the isolates of *Salmonella enteric* strains as explained by (Saravanan *et al*., 2018) with slight modifications. The vancomycin (30 µg) was used as standard. The sample and the standard antibiotic were placed on Mueller Hinton agar plate's inoculated with 100 µl, 1×10^5 of the bacterial suspension. The plates were incubated for 18-24 h at 37□. Zone of inhibition of the NHD and NHD-AgNPs were measured.

Alamar blue antibacterial assay

Stock solutions of compound and its nanoparticles ranging concentration from (10-160µg/ml) was prepared in distilled water and placed in 96 well plate such that their final volume becomes 100µL (compound + media). Fully grown turbid (*Salmonella enterica* subsp. *Enterica* serovar Typhimurium (ATCC 700408 and ATCC 14028)) were 1000 times diluted in media and 100µL of this diluted bacterial media were added to all previous wells such that final volume (200µL) would contain bacterial load approximately ($0.5\text{-}1.0 \times 10^6$cfu/mL). Positive control contains only media and bacteria. Each concentration was run in triplicates. The sealed plates were further incubated 18-22 hrs at 37□. Next day, all wells were visually checked to know the growth of bacteria. Soon after noticing the clear and turbid wells, the RS salt dye to each well (Che-Ipex-Int'LInc) 20µL of 0.02% was added, and further the plate was incubated with shaking at 80 rpm, and 37□ for 2-hrs. For quantitative analysis, absorbance was measured at 570 nm and 600 nm in Multiskn™ GO spectrophotometer (Thermo Scientific, USA). The bacterial growth inhibition percentage was calculated accordingly.

Surface morphological analysis (AFM)

Fully grown bacteria (*Salmonella enterica* subsp. *Enterica* serovar Typhimurium ATCC 700408 and ATCC 14028 were diluted and adjusted to approximate turbidity of 0.5 McFarland index (1.5×10^8cfu/mL). These cells were treated with compound and its nanoparticle (100 µM) and subjected to incubation at 37°C for 18-20 hrs. After incubation, the cells were centrifuged (3000 rpm for 5 min). The cells were subjected twice to washing through analytical grade water. The NHD, NHD-AgNPs treated as well as control bacterial cells were treated with 0.01% poly-L-lysine and then about 10-µl were applied on mica slide surfaces explained by (Shah *et al*., 2014). The slides were dried at ambient temperature and images of bacteria cells were obtained on atomic force microscope (AFM) (Agilent Technologies 5500). Topography and pseudo color images were obtained after each scan, and images were analyzed using (Pico View 1.2) software.

STATISTICAL ANALYSIS

Data was statistically analyzed using GraphPad Prism 6.lnk software. Data is expressed as mean± standard error mean. One-way ANOVA was used, statistical significance was contemplated at *p<0.05, **p<0.01 and ***p<0.001.

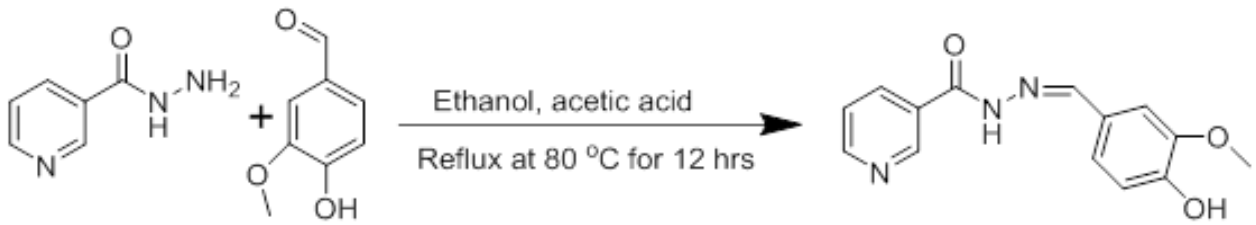

Synthesis scheme: Schiff base (NHD) of 4-hydroxy-3-methoxybenzaldehyde with nicotinic hydrazide

Table 1: Zone of inhibition of NHD and NHD-AgNPs against *S. enterica* (ATCC 14028 and ATCC 700408) using disc diffusion method.

Antimicrobial agent	Disc concentration (µg/mL)	*Salmonella enterica* ATCC 14028	*Salmonella enterica* ATCC 700408
		Zone of inhibition (mm)	Zone of inhibition(mm)
NHD	160	48.01 ±1.43**	45.29 ±1.66**
NHD -AgNPs	130	55.87 ±2.08***	52.88 ±1.42***
Vancomycin	30	33.00 ±1.45**	28.63 ±1.43*

Table 2: MIC of NHD and NHD-AgNPs against *S. enterica* (ATCC 14028 and ATCC 700408) using Alamar Blue assay

Antimicrobial agents	*Salmonella enterica* (ATCC 14028)		*Salmonella enterica* (ATCC 700408)	
Compound	MIC	% inhibition using Alamar Blue dye	MIC	% inhibition using Alamar Blue dye
NHD	85µg/ml	75±3.55**	150 µg/ml	70±4.10**
NHD-AgNPs	75µg/ml	80±3.45***	125 µg/ml	75±4.05**
Vancomycin	30 µg/mL	62±3.15*	30 µg/mL	55±1.06*

Values are expressed as mean±SEM, of nicotine hydrazide derivative (NHD) and its AgNPs against *S. enterica* ATCC 14028 and ATCC 700408. Vancomycin was used as standard, for statistical evaluation one-way ANOVA followed by post hoc test was performed at (*p<0.05, **p<0.01, ***p<0.001)

RESULTS

Cytotoxicity against normal 3T3 cell line

The newly synthesized Schiff base derivative of nicotinic hydrazide (NHD) and its silver capped nanoparticles were evaluated against normal mouse (3T3) fibroblast cells. NHD produce ≈LD_{50} at >1000µg/mL as shown in (fig. 6). The nicotinic hydrazide derivative nanoparticles (NHD-AgNPs) did not show any toxicity at 1000µg/mL. The probable LD_{50} might be >1500µg/mL.

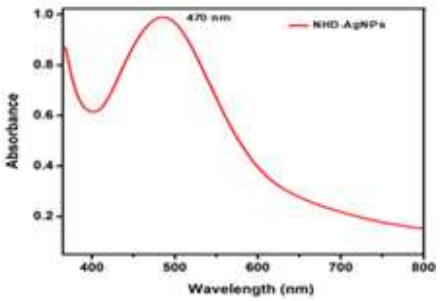

Fig. 1: UV-Visible absorbance spectrum of Schiff base NHD- AgNPs at 470 nm.

Antibacterial activity using disc diffusion method

S. enterica treated with NHD showed more than 45.29 ±1.66 and 48.01±1.43 mm zone of inhibition against both strains (ATCC 14028, ATCC 700408) at maximum concentration of 160µg/mL (p<0.01). On the other hand, NHD-AgNPs showed 55.87±2.08 and 52.88±1.42 mm zone of inhibition against *S. enterica* ATCC 14028 and *S. enterica* ATCC 700408 at maximum concentration of 130 µg/mL (p<0.001). Standard drugs vancomycin showed moderate zone of inhibition against both strains on as depicted in table 1. The results of silver decorated NHD were compared with standard drug vancomycin.

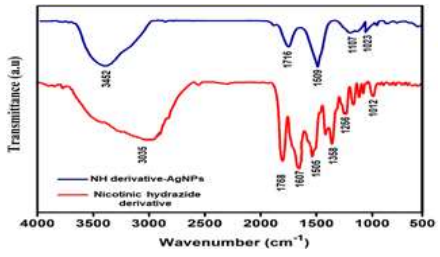

Fig. 2: FTIR spectrum of Schiff base NHD (red trace) and NHD–AgNPs (blue trace)

Alamar blue antibacterial assay

On treating *S. enterica* bacteria with NHD and NHD-AgNPs displayed inhibition >70% for both sensitive (ATCC 14028) and MDR strain (ATCC 700408). MIC concentration of nicotinic hydrazide Schiff base was 85

and 150 µg/ml against (ATCC 14028) and MDR strain (ATCC 700408) respectively ($p<0.01$), while its AgNPs MIC was 75 and 125µg/ml (ATCC 14028) and MDR strain (ATCC 700408) at ($p<0.001$). Standard drug vancomycin also showed significant ($p<0.05$) resistant against these strains table 2. The results of NHD-AgNPs were compared with standard drug vancomycin.

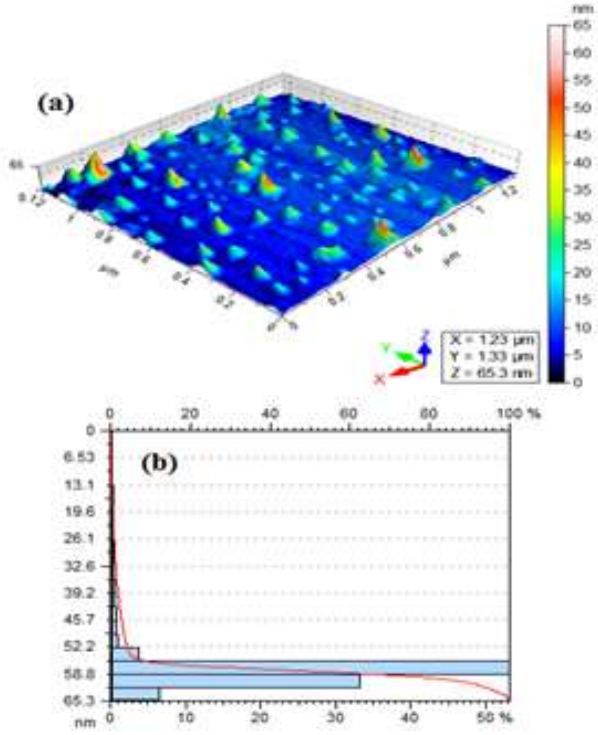

Fig. 3: AFM analysis of Schiff base coated silver nanoparticles (a) 3D-Topographical image and (b) average particles height graph

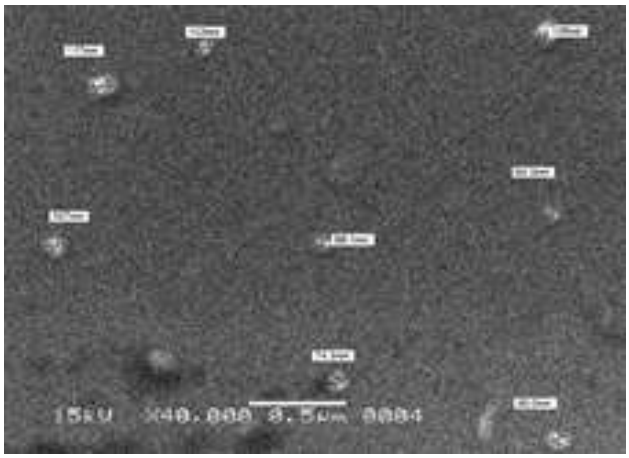

Fig. 4: SEM analysis of silver nanoparticles of NHD at magnification of x40,000

AFM study of S. enterica

AFM study was performed to find the surface topography of the *S. enterica* (ATCC 14028 and ATCC 700408) by scanning in tapping mode. The length and width of untreated *S. enterica* of both strains were found in the range of 2-5µm and 0.7-1.8µm respectively (fig. 7A-D). Untreated cells were non-encapsulated and in rod shape with smooth surface without sign of cytoplasmic leakage. Due to overcrowding of cells, flagella were not properly seen. Whereas, upon treatment *S. enterica* (ATCC 14028 and ATCC 700408 with nicotinohydazide Schiff base derivative (fig. 8A and 8D) and its nano-particle (fig. 8B and 8E), affected cells were severely damaged. The cytoplasmic content appeared to be leaked from the cells. Flagella of many cells could be seen scattered after separating out from the ruptured cells. Vancomycin treated bacterial images are reflected in fig. 8C and 8F.

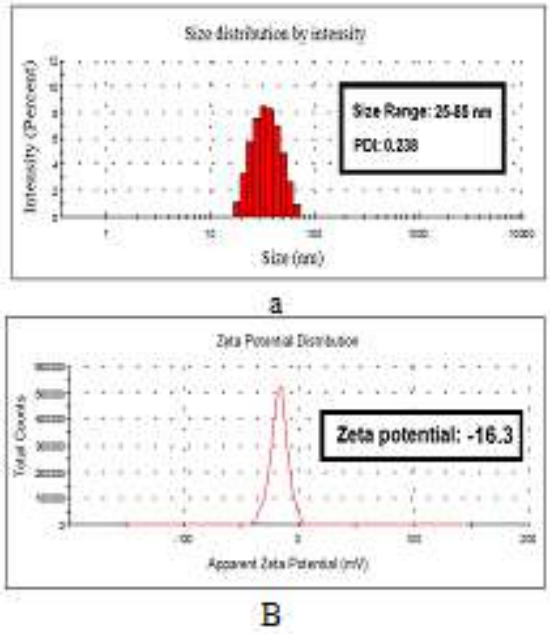

Fig. 5: (a) Dynamic light scattering (DLS) histogram showing the average particle size distribution of Schiff base derivative of NH coated AgNPs (b) Zeta potential

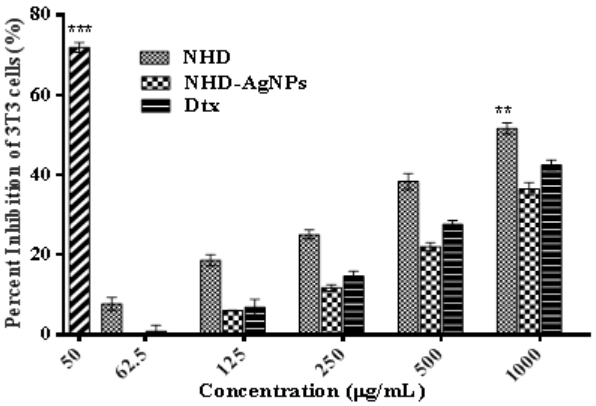

Fig. 6: Percent cell cytotoxicity of nicotine hydrazide derivative (NDH) and its sliver nanoparticles (NHD-AgNPs) against 3T3 call line. Dtx (Docetaxel), results are presented as mean ± SEM at (*$p<0.05$, **$p<0.01$, ***$p<0.001$) after applying one-way ANOVA followed by post hoc test

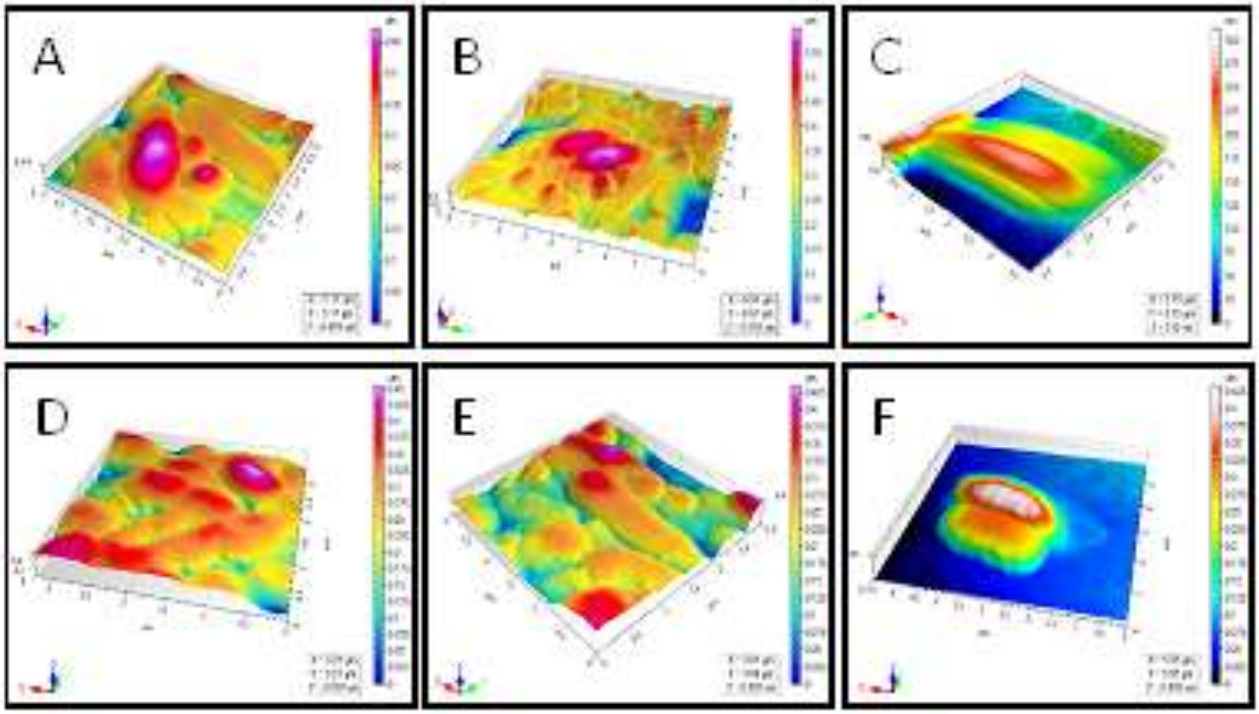

Fig. 7: Untreated control of *Salmonella enterica*ATCC 700408 (A,B,C) and ATCC 14028 (D,E,F)

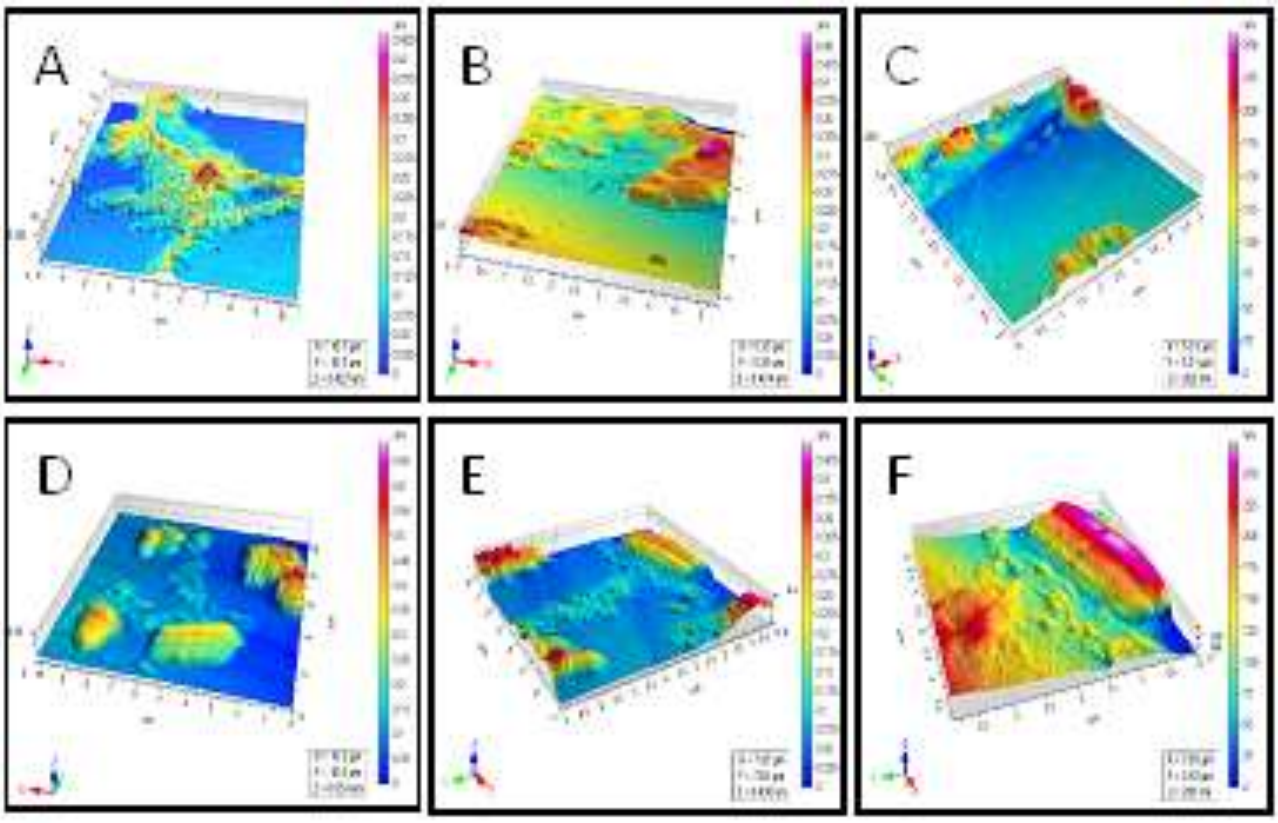

Fig. 8: (A, D) *S. enterica* ATCC 700408 and ATCC 14028 treated with NHD at 160 µg/ml, (B, E) *S. enterica* ATCC 700408 and ATCC 14028 treated with NHD-AgNPs at 130 µg/ml, (C, F) *S. enterica* ATCC 700408 and ATCC 14028 treated with vancomycin at 30 µg/ml

DISCUSSION

Even if there have been several studies done over the last decade for the discovery of novel antibacterial agent the emerging resistance by pathogens to existing chemotherapeutic agent evoke researchers to synthesize new, safe and effective antibacterial agent (Tsemeugne *et al*., 2018). Schiff bases among several synthetic compound grab amazing position in the pharmaceutical arena (Naganagowda *et al*., 2014). Moreover, the nano-fabrication of synthesized compounds aid a unique physicochemical property to the existing or newly synthesized molecules. Particularly AgNPs efficiently deliver molecule through bacterial cell wall via conjugation of AgNPs with bacterial cell surface, this will enhance antibacterial activity and kinetics against resistant gram negative pathogens (Shah *et al*., 2014). With these views, in current study a novel Schiff base derivative of nicotinic hydrazide was tailored. The nicotinic hydrazide was capped with silver nanoparticles and characterized as explained by (Gade *et al*., 2010). The NHD-AgNPs exhibit peaks at 460 nm. Significant stretching vibrational peaks were observed at 1700cm^{-1} and 1607 cm^{-1} which corresponded to the presence of C=O and C=C groups, respectively (Ramasamy *et al*., 2017). After the formation of NH derivative-Ag nanoparticles, peak shifts were observed in the spectrum. Peaks appearing at 1716 cm^{-1} and 1509 cm^{-1} indicated the involvement of -CHO group in the stabilization of nanoparticles (Ramasamy *et al*., 2017). 3035cm^{-1} conforms (OH) on benzene in red trace, starched to 3452 after AgNPs blue trace. The particle size and morphology being an important parameter of nano- architected drugs provide physical stability and *in vivo* performance (Rao *et al*., 2017). The average particle size (55-65 nm) is technically well placed as previously (Singh and Lillard Jr, 2009). Among various electron microscopic techniques, SEM is capable of resolving particle size, size distribution, shape and surface morphology of synthesized nanomaterial (Lin *et al*., 2014). The NHD-AgNPs average size was 96.55 nm. Zeta potential another important parameter with negative charge are preferred as physically stabled. NHD-AgNPs anticipate a significant interaction of molecule with bacterial cell surface.

The nicotinic hydrazide Schiff base derivative significantly inhibited *S. enterica* (ATCC 14028 and ATCC 700408) growth via producing a broad zone of inhibition at maximum concentration of 160µg/mL. The NHD-AgNPs more efficiently inhibited bacterial growth at 130µg/mL, which was reflected by broader zone of inhibition. The NHD-AgNPs achieved maximum inhibition at lower concentration then NHD. The results suggest that the NPs are more active against both strains of *S. enterica* as compare to NHD. Compared to NHD all the NPs were more bactericidal, this may be due to synergistic effect of NHD and AgNPs. Our results are reconciled with the zone of inhibitions reported in (Wikler, 2006), moreover the results were comparable with standard vancomycin. The significant antibacterial performance of NHD and its nanoparticles were further authenticated via AFM study. The untreated bacterial cells of *S. enterica* both strains exhibited regular normal smooth cell membrane with length and width in the range of 2-5 µm and 0.7-1.8µm respectively, which were similar to the reported results (Aytac *et al*., 2003). On the other side the bacterial cells treated with NHD, induce cell rapture of both *S. enterica* (ATCC 14028 and ATCC 700408) significantly. Comparative to nicotinic hydrazide derivative treated *S. enterica* species, NHD-capped AgNPs showed increased degradation of bacterial cell wall. The high resolution and three-dimensional images of bacterial cells provided a detailed topographical description of antibacterial effect of NHD derivative and NHD capped AgNPs. Silver nanoparticles can easily adhere to the bacterial cell membrane owing to high affinity of Ag toward Sulfur. Inside cell penetration the drugs can disturb bacterial DNA and vital organelles that could possibly interrupt vital cellular functions (Rai *et al*., 2009, Feng *et al*., 2000,Sondi and Salopek-Sondi, 2004, Morones *et al*., 2005 and Song *et al*., 2006). These results showed that silver capped nanoparticles of Schiff base synthesized compound were highly active against both sensitive and MDR strains of *S. enterica* at their MIC concentration. In future, the synthesized compound and its AgNPs will be considered for wound healing activity.

CONCLUSION

The newly synthesized Schiff base nicotinic hydrazide derivative and its nano particle's antibacterial activity was evaluated by disk diffusion and Alamar Blue assay method against two strains of *S. enterica.* The silver nanoparticles of derivative of Schiff base nicotinic hydrazide showed good inhibition against both, sensitive and MDR strains of *S. enterica*. Due to its good anti-*salmonella activity* and less cytotoxic nature. It could be a good candidate as anti-typhoid agent and can be further evaluated for its mechanistic studies.

REFERENCES

Aytac S, Mercanoglu B, Ergun M and Tan E (2003). The visualisation of *Salmonella enteritidis* by atomic force microscopy. *Ann. Microbiol.*, **53**(3): 337-342.

Burki S, Mehjabeen, Burki ZG, Jahan N, Muhammad S, Mohani N, Siddiqui FA and Owais F (2019). GC-MS profiling, FTIR, metal analysis, antibacterial and anticancer potential of *Monotheca buxifolia* (Falc.) leaves. *Pak. J. Pharm. Sci*., **32**(5): 2405-2413.

Donlan RM (2002). Biofilms: Microbial life on surfaces. *Emerg. Infect. Dis.*,**8**(9): 881.

Eldehna WM, Fares M, Abdel-Aziz MM and Abdel-Aziz HA (2015). Design, synthesis and antitubercular

activity of certain nicotinic acid hydrazides. *Molecules.,* **20**(5): 8800-8815.

Fauci AS, Touchette NA and Folkers GK (2005). Emerging infectious diseases: A 10-year perspective from the National Institute of Allergy and Infectious Diseases. *Int. J. Risk. Saf. Med.,* **17**(4): 157-167.

Feng QL, Wu J, Chen G, Cui F and Kim Tand Kim J (2000). A mechanistic study of the antibacterial effect of silver ions on *Escherichia coli* and *Staphylococcus aureus*. *J. Biomed. Mater. Res.,* **52**(4): 662-668.

Gade A, Gaikwad S, Tiwari V, Yadav A, Ingle A and Rai M(2010). Biofabrication of silver nanoparticles by Opuntia ficus-indica: *in vitro* antibacterial activity and study of the mechanism involved in the synthesis. *Curr. Nanosci.,***6**(4): 370-375.

Guo Z, Xing R, Liu S, Zhong Z, Ji X, Wang L and Li P(2007). Antifungal properties of Schiff bases of chitosan, N-substituted chitosan and quaternized chitosan. *Carbohydr. Res.,* **342**(10): 1329-1332.

Gurunathan S(2014). Rapid biological synthesis of silver nanoparticles and their enhanced antibacterial effects against *Escherichia fergusonii* and *Streptococcus mutans*. *Arab. J. Chem.,***12**(2): 168-180.

Kajal A, Bala S, Kamboj S, Sharma N and Saini V(2013). Schiff bases: A versatile pharmacophore. *J. Catal.,* pp.1-14.

Karthikeyan MS, Prasad DJ, Poojary B, Bhat KS, Holla BS and Kumari NS (2006). Synthesis and biological activity of Schiff and Mannich bases bearing 2, 4-dichloro-5-fluorophenyl moiety. *Bioorg. Med. Chem.,* **14**(22): 7482-7489.

Lin PC, Lin S, Wang PC and Sridhar R (2014). Techniques for physicochemical characterization of nanomaterials. *Biotechnol. Adv.,* **32**(4): 711-726.

Marasini BP, Baral P, Aryal P, Ghimire KR, Neupane S, Dahal N, Singh A, Ghimire L and Shrestha K (2015). Evaluation of antibacterial activity of some traditionally used medicinal plants against human pathogenic bacteria. *Biomed. Res. Int.,* pp.1-6.

Morones JR, Elechiguerra JL, Camacho A, Holt K, Kouri JB, Ramírez JT and Yacaman MJ (2005). The bactericidal effect of silver nanoparticles. *Nanotechnology.,***16**(10): 2346.

Naganagowda G, Meijboom R and Petsom A (2014). Synthesis and antimicrobial activity of new schiff base compounds containing 2-hydroxy-4-pentadecylbenzaldehyde moiety. *Adv. Carbohydr.,* 1-9.

Przybylski P, Huczynski A, Pyta K, Brzezinski B and Bartl F (2009). Biological properties of Schiff bases and azo derivatives of phenols. *Curr. Org. Chem.,***13**(2): 124-148.

Rai M, Yadav A and Gade A(2009). Silver nanoparticles as a new generation of antimicrobials. *Biotechnol. Adv.,* **27**(1): 76-83.

Ramasamy M, Lee JH and Lee J (2017). Direct one-pot synthesis of cinnamaldehyde immobilized on gold nanoparticles and their antibiofilm properties. *Colloids. Surf. B. Biointerfaces.,***160**: 639-648.

Rao K, Imran M, Jabri T, Ali I, Perveen S, Ahmed S and Shah MR (2017). Gum tragacanth stabilized green gold nanoparticles as cargos for Naringin loading: A morphological investigation through AFM. *Carbohydr. Polym.,* **174**: 243-252.

Saravanan M, Barik SK, Mubarakali D, Prakash P and Pugazhendhi A (2018). Synthesis of silver nanoparticles from Bacillus brevis (NCIM 2533) and their antibacterial activity against pathogenic bacteria. *Microb. Pathog.,* **116**: 221-226.

Shah MR, Ali S, Ateeq M, Perveen S, Ahmed S, Bertino MF and Ali M (2014). Morphological analysis of the antimicrobial action of silver and gold nanoparticles stabilized with ceftriaxone on *Escherichia coli* using atomic force microscopy. *New J Chem.,* **38**: 5633-5640.

Singh R and Lillard Jr JW (2009). Nanoparticle-based targeted drug delivery. *Exp. Mol. Med.,* **86**(3): 215-223.

Sondi I and Salopek-Sondi B (2004). Silver nanoparticles as antimicrobial agent: a case study on *E. coli* as a model for Gram-negative bacteria. *J. Colloid. Interface. Sci.,***275**(1): 177-182.

Song H, Ko K, Oh I and Lee B (2006). Fabrication of silver nanoparticles and their antimicrobial mechanisms. *Eur. Cell. Mater.,***11**(6): 58.

Souza AOD, Galetti F, Silva C L, Bicalho B, Parma MM, Fonseca, SF, Marsaioli AJ, Trindade AC, Gil RPF and Bezerra FS (2007). Antimycobacterial and cytotoxicity activity of synthetic and natural compounds. *Quim. Nova.,***30**(7): 1563-1566.

Tsemeugne J, Sopbue Fondjo E, Tamokou, JDD, Rohand T, Ngongang AD, Kuiate JRand Sondengam BL(2018). Synthesis, Characterization, and Antimicrobial Activity of a Novel Trisazo Dye from 3-Amino-4H-thieno [3, 4-c][1] benzopyran-4-one. *Int. J. Med. Chem.,***2018**: 1-8.

Vicente M, Hodgson J, Massidda O, Tonjum T, Henriques-Normark B and Ron EZ (2006). The fallacies of hope: will we discover new antibiotics to combat pathogenic bacteria in time? *FEMS Microbiol. Rev.,***30**(6): 841-852.

Wikler MA (2006). Performance standards for antimicrobial susceptibility testing Sixteenth informational supplement. *M 100-S 16.*

Wingender J and Flemming H (2010). The biofilm matrix. *Nature. Rev. Microbiol.,***8**(9): 623-633.

Wu D, Fan W, Kishen A, Gutmann JL and Fan B (2014). Evaluation of the antibacterial efficacy of silver nanoparticles against *Enterococcus faecalis* biofilm. *J. Endod.,***40**(2): 285-290.